Examination of scoring parameters of corrugated fiberboard

JOHN M. CONSIDINE, NATHAN J. BECHLE, JAMES J. BRIDWELL, MATTHEW ARVANTIS, BENJAMIN FRANK, AND XIAOYAN TANG

ABSTRACT: One of the less interrogated aspects of corrugated packaging are scoring and scoring profiles, the intentional localized crushing of flutes to accommodate package folding and closure. This study explores the effect of scoring parameters on box compression test strength (BCT) of two balanced corrugated boards.

Scoring differences produced BCT that varied by 10% for one board and less for the other board. Parameters from 4-point bending of scored specimens showed some correlation with BCT, while eccentricity and torsion parameters had less correlation. Different scores produced BCT differences that were not strongly predicted by most standard tests in the current study, implying other tests may be needed to examine the actual boundary conditions on a box during compression. In a few cases, aggressive scoring produced cracked score lines, and those containers had lower BCT than containers with uncracked score lines.

Application: This study is the first to directly compare the impact of different flap scoring profiles on box compression strength. The impact of score cracking on box performance was clearly seen, with other impacts depending on material and requiring further exploration.

Corrugated paperboard packaging is the primary material used to ship goods around the world. For more than 100 years, corrugated boards have been modified and improved to protect products during transportation. It is a green material that is renewable, recyclable, reusable, and biodegradable. Furthermore, it is lightweight and is effective at protecting a wide variety of products, from produce to electronics to medical equipment. Corrugated packaging is a commodity material in a mature industry that contributed US$224 B to the U.S. economy in 2023 [1]. Paper mills, which produce linerboards (outer faces in corrugated board) and mediums (inner corrugated material), and corrugating plants are expensive to build and maintain. Changes to processes need to demonstrate significant savings (10% improvement is a common benchmark) or competitive advantages before implementation. The primary performance metric for corrugated containers is box compression test strength (BCT). McKee et al. [2] developed a model to estimate BCT by modeling the elastic buckling of the four vertical panels for a box. Parameters were determined by fitting to BCT data for boxes, without examining how the scores and flaps impact the loading geometry and resulting BCT.

The compressive strength of tubes is higher than those of similar boxes with flaps [3-5]. For large boxes, Angell and Paslay [6] found tubes to have 40% greater BCT compared to boxes. Kutt and Mithel [7] proposed a grooved scoreline for containers that had 20% higher BCT than those boxes with regular scores. Performing cold scoring with different scoring parameters and comparing with the customary scoring profile on the same material, their alternative scoring profiles created boxes that had -9.5% to +13.5% changes in BCT. They note that light scoring, which is small damage to the corrugated flutes, produced less defined fold lines and reduced BCT. Garbowski et al. [8] showed between 3%–18% difference in BCT with different scoring parameters. Large data sets of BCT exist but do not contain information on scoring [9]. Koning and Laundrie [10] state "the negative effect of scorelines on box compression is not fully quantified nor understood, and we are challenged either to eliminate the effect or to develop a new material that is not damaged by scoring." Reinforcing the need for more study, Frank [11] states: "However, given the differences in strength noted in the literature, with tubes anywhere from 10% to 90% stronger than similarly constructed boxes, there is ample motivation to explore scoring profiles and attempt to capture more of the improved performance of a tube structure in the design of boxes." The objective of this work is to examine the effect of scoring parameters, that is, scoring geometry, depth, and offset, on BCT.

Recent equipment development has made this investigation more relevant, as modern corrugating operations are able to easily change different scoring parameters (including depth, offset, and style) as needed for each order. Moreover, material utilization within the packaging industry has transitioned from virgin materials to a large percentage of recycled materials, and new data is needed to motivate processing changes. It is generally assumed that flaps create eccentric loading of the box panels that reduce maximum panel strength and contribute to the total deformation of the container [12]. Up to 90% of total deflection during BCT is attributed to score lines [5]. Peterson and Schimmelpfenning [13] documented rotation at score lines during loading to show that a different boundary condition exists than that assumed in the McKee model and demonstrated that eccentric loading reduced BCT. It has been shown that eccentric loading of plates causes failure at lower buckling forces than plates without eccentric loading [14], and Angell and Paslay [6] stated that initial eccentricity greatly reduces buckling load. Nordstrand [15] created a finite element model (FEM) to examine several factors of corrugated construction. His model showed 15% loss of maximum load when eccentricity is as low as one-quarter of the board thickness. Discrepancies between FEM and experiments are often attributed to score line behavior that is not included in the modeling [16].

Due to the large parameter space, this work is exploratory. We report the BCT of one size of regular slotted container (RSC) boxes made from two board constructions and scored with a variety of geometries, depths, and offsets, in order to qualitatively assess the scale of the impact arising from changing scoring parameters. In addition to the standard testing of component materials and combined board, we performed testing to examine the score line behavior and used statistical modeling to assess their impacts on BCT.

MATERIALS

This study focused on two balanced C-flute board combinations, using a pair of nominal 250 g/m² liners combined with a nominal 112 g/m² medium (B1) and a pair of nominal 160 g/m² liners with a nominal 112 g/m² medium (B2). The two combinations were produced on the same corrugator, varying the corrugator scores as needed to produce 10 sets of boxes from each. **Table I** identifies the labels for

Score	Label
Light 3 Point	L3
3 Point	3P
Heavy 3 Point	H3
Light Point-to-Point	LP
Point-to-Point	PP
Heavy Point-to-Point	HP
Light Offset	LO
Offset	OF
Heavy Offset	HO
Beer	BS
Unscored/No Score	NS

I. Scoring identification and labels for the different

the evaluated scoring profiles, which resulted in 19 different material designations (B2 HP was not produced). For B1, the scores H3, HP, and HO had cracked inside liner. For B2, score H3 had a cracked liner at the score. All other materials matched the requirements of boxes fit-for-use [17]. Because of the balanced board structure, we expect the eccentricity measurements described in the following sections to be primarily or entirely a function of the scoring profile and residual stresses, and not a function of board structural parameters, which might be the case for board comprised of two different weight liners.

TESTING

Typical test properties

Caliper, edgewise compression test (ECT), and bending stiffnesses for the two materials are listed in **Table II**. Caliper of each material was measured according to TAPPI Standard Test Method T 411 "Thickness (caliper of paper, paperboard, and combined board)," using 50 measurements per specimen. The ECT strength was performed using the clamp method according to TAPPI T 839 "Edgewise compressive strength of corrugated fiberboard using the clamp method (short column test)." Tests were rejected that failed within the clamped region and specimens were cut from unscored sheets.

Four-point bending stiffness was evaluated using the classical method, TAPPI T 820 "Flexural stiffness of corrugated board," for flexural stiffness of corrugated board. We used the four-point geometry because the boundary conditions, supports, and load application regions produce less localized stress and avoid clamping issues. The outer span was 228 mm, and inner span was 114 mm. Mid-point deflection was measured with a linear variable differential transformer (LVDT). Overall length of the specimens was 279 mm, and width was 51 mm. Load, span displacement, and mid-point displacement were captured at 10 Hz. Four-point bending tests were performed on unscored board, as well as on scored fiberboard specimens, for the CD, as shown in **Fig. 1** and **Fig. 2**, using the same geometry and test method as that for the unscored board. Bending results for the scored board were used to assess score behavior

	B1		B2	
	μ	σ	μ	σ
Caliper, mm	4.43	0.02	4.14	0.02
ECT, kN m^{-1}	7.62	0.39	5.52	0.22
Bending stiffness (Nm) MD	13.08	0.22	7.95	0.11
CD	8.31	0.21	5.84	0.08

II. Average (μ) and standard deviation (σ) of caliper, ECT, and bending stiffnesses for each board.

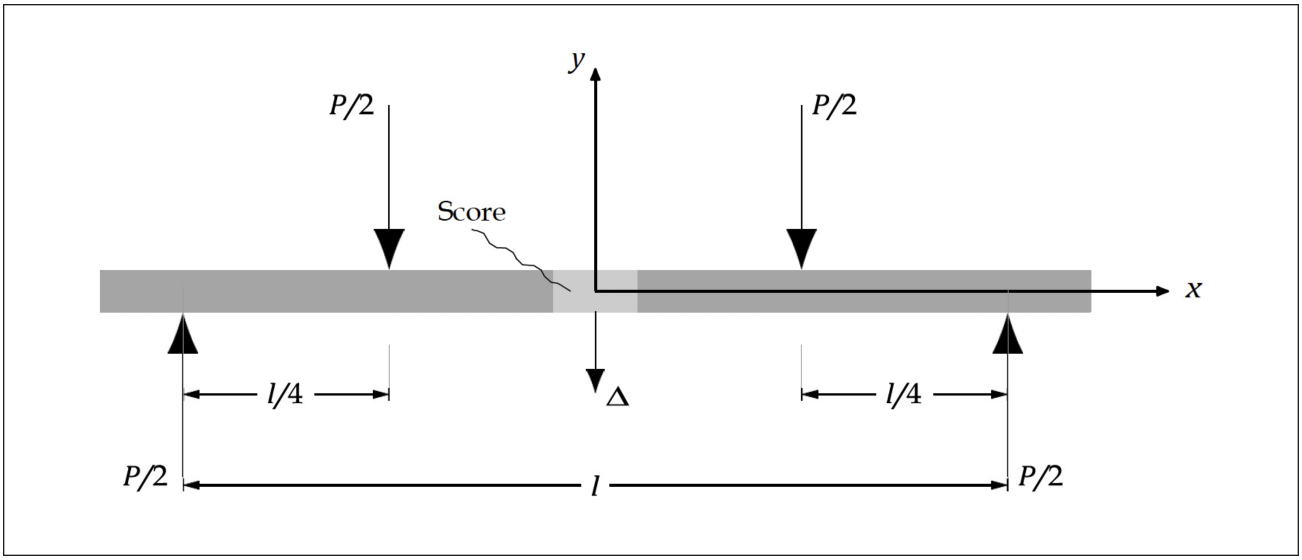

1. Schematic of 4-point bending test (l = length between lower supports, effective length of specimen, 228 mm; P = total applied force; Δ = central point deflection as measured with a linear variable differential transformer, LVDT).

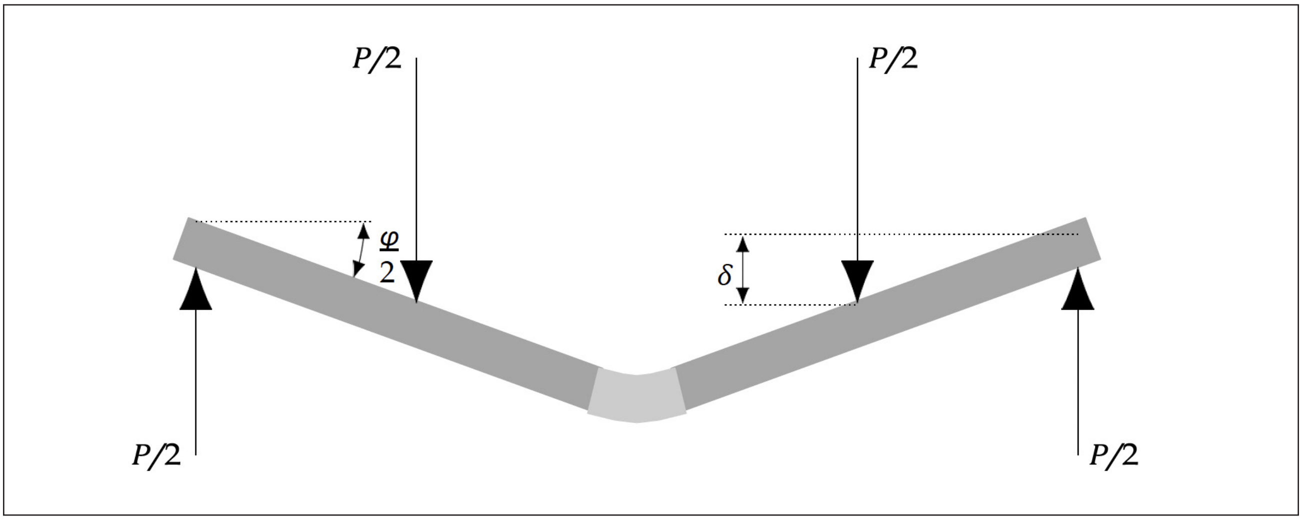

2. Schematic of 4-point bending test showing half the rotation of each section of board, measured from horizontal (φ) and deflection of the load application point (δ).

and provide some qualitative information of the boundary conditions for BCT. To evaluate flexural stiffness at the score, the specimen was placed on the bending fixture such that the score was located at mid-span, i.e., equidistant from each support. Traditionally, bending moment resistance for a cantilever geometry has been used to evaluate the score behavior of cartonboard [18-23].

Bending tests were plotted using bending resisting moment at the score, K, and φ as given by:

$$K = \frac{Pl}{8} \quad (1)$$

$$\varphi = tan^{-1}\frac{4\delta}{l} \quad (2)$$

where:

K: bending resisting moment at the score
P: total applied force
l: length between lower supports, effective length of specimen, 228 mm
φ: half the rotation of each section of board, measured from horizontal
δ: displacement of the crosshead of machine at $\frac{l}{4}$

Figure 3 shows a representative score bending test and the identified parameters. Inflection was found by using a smoothing spline for the data after K_{max} and locating the slope closest to 0°. The initial slope, $\frac{dK}{d\varphi}$, was calculated by a linear regression of the data where $K \geq 30$ such that the

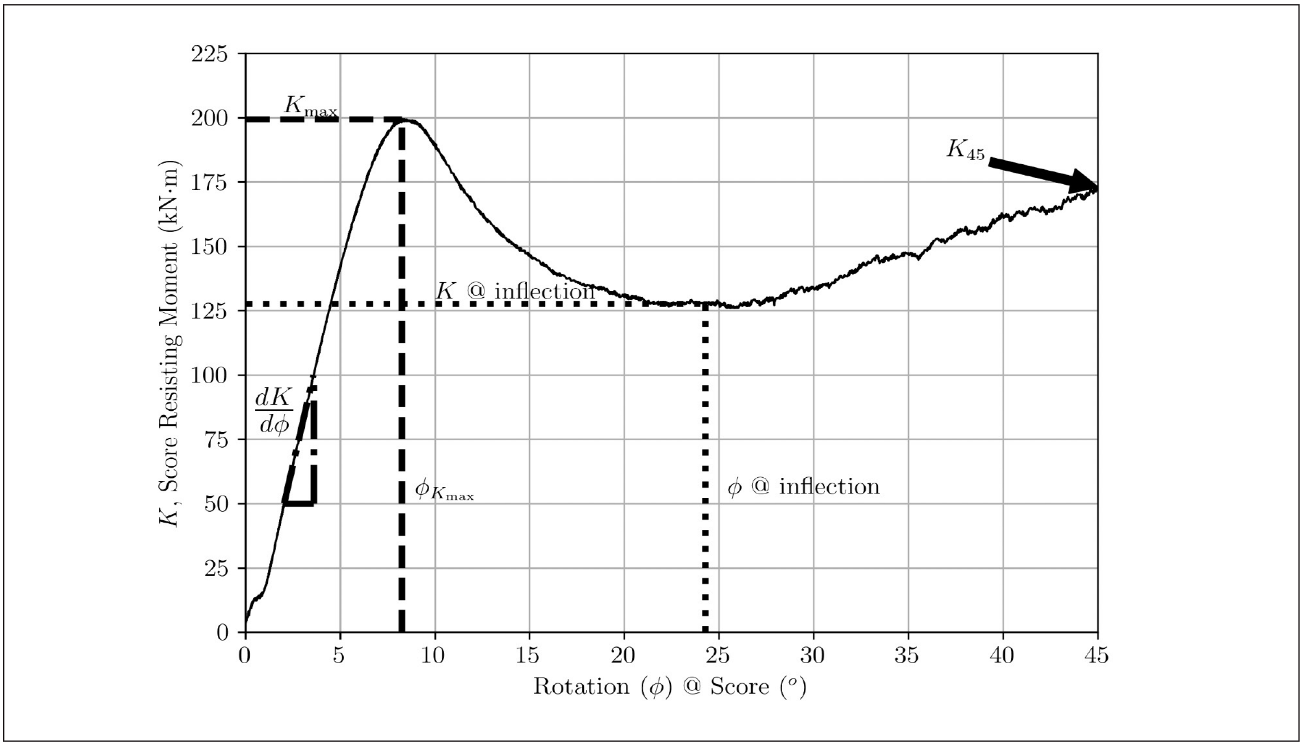

3. Example 4-point bending test showing identified parameters (K: bending resisting moment at the score; $\frac{dK}{d\varphi}$: initial slope, K_{45}: stiffness at φ =45, where φ is given in Eq. 2).

$r^2 \geq 0.99$ (r^2: coefficient of determination).

Torsional stiffness

Torsional stiffness of specimens containing a score line were tested in a Chalmers C1 dynamic stiffness tester (DST) (Korutest Limited; Roturua, NZ). This equipment tests a corrugated board specimen that is 145-mm long and 25-mm wide with an active length of 100 mm. Initial rotation of the specimen is 5°. The device identifies the angular natural frequency of the specimen according to Eq. 3 [24]. All specimens were oriented with machine direction (MD) along the long axis of the specimen. **Figure 4** shows the DST specimen with its score line location. The output of the equipment is $\omega^2/100$, which we call DST, and assumes I is a constant. Thus, the test allows comparison only between boards of the same material and construction.

$$T = I\omega^2 \quad (3)$$

where:
T: torsional stiffness
ω: angular natural frequency
I: moment of inertia of the system

This device was designed to measure loss of torsional stiffness due to glue line skips, which are areas with less or no bonding between the fluting medium and the linerboard. Its use here examines the loss of torsional stiffness due to scoring.

Eccentricity

Eccentricity was measured on a device patterned after one described by Renman [25], shown in **Fig. 5**, and is defined as the horizontal distance from the center of the vertical box panel to the load application, denoted as e. Nominal dimensions for eccentricity specimens featured a 191-mm horizontal leg, 64-mm vertical leg, and 51-mm width. The fixture was installed in an Instron 5544 electromechanical universal test frame (Instron; Norwood, MA, USA). A 2 kN-capacity Instron Model 2530-418 load cell was used to measure the force, P, resisted by the test frame crosshead. A 110 N-capacity Sensotec Model 41 load cell (Honeywell; Charlotte, NC, USA) was used to measure the force, P_2, at the end of a steel bar that could freely pivot about a point above the center of the vertical clamp aligned with the crosshead motion.

Equilibrium of vertical forces acting on the fixture yields Eq. 4:

$$P_1 - P_2 - P = 0 \quad (4)$$

Similarly, moment equilibrium about the pivot point yields Eq. 5:

$$MR - P_1 e - P_{2a} = 0 \quad (5)$$

Residual moment (MR) tests were performed by measuring the load at P_2 with 1) no specimen installed, and 2) after

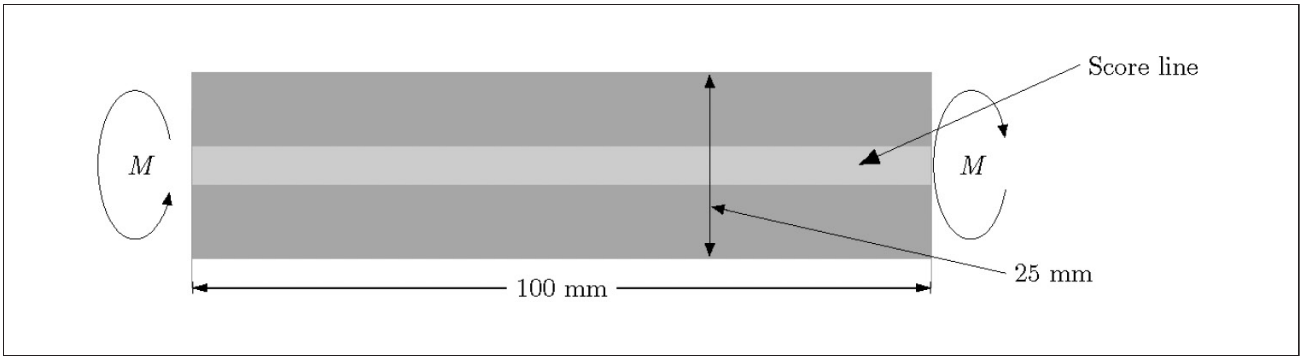

4. Schematics of machine direction (MD) dynamic stiffness tester (DST) specimen. The* M *denotes applied moment.

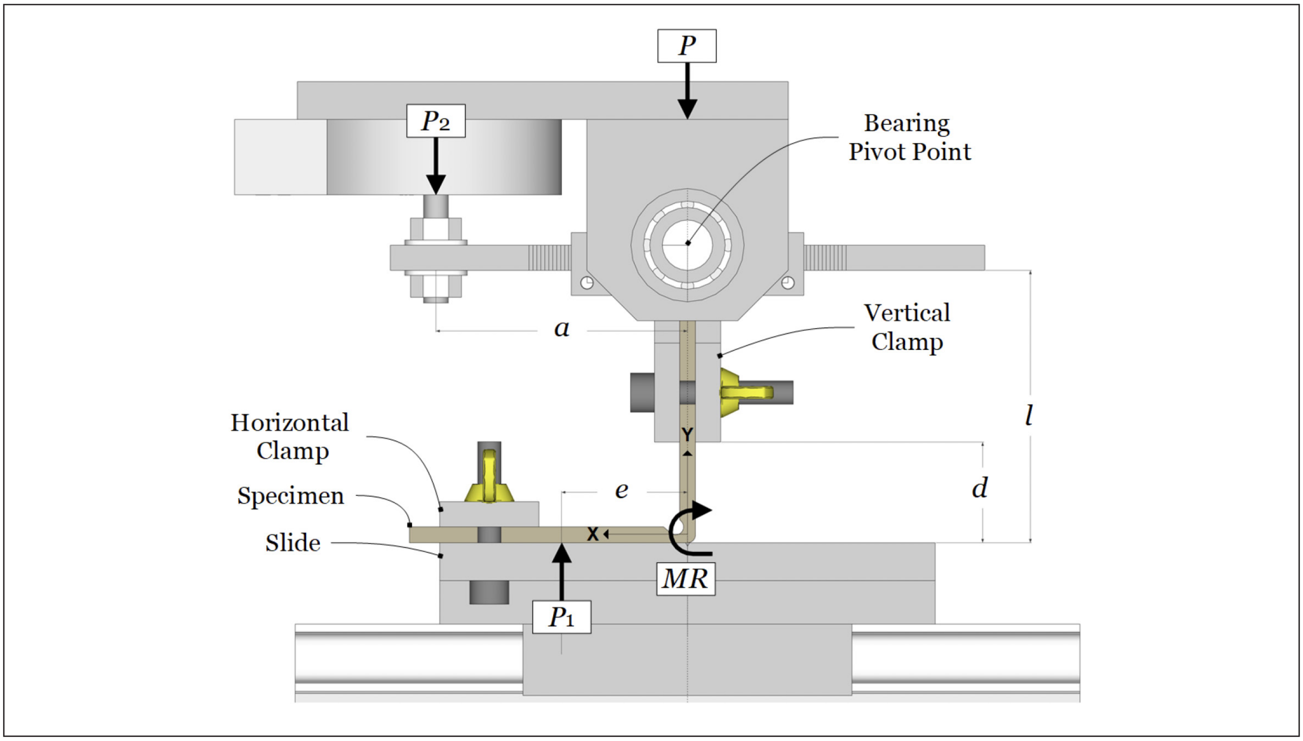

5. Diagram of the eccentricity (*e*) fixture. Eccentricity is measured from the center of the board to the interior of the box. The extent of* e *is exaggerated for visualization; more typically, the eccentricity falls within the thickness of the board specimen, especially near failure (*MR*: residual moment).

a specimen was placed in the fixture and folded to 90° with the vertical leg unclamped. The measured difference between the readings was taken as the contribution of the residual moment to the load measured at P_2. After taking the initial residual moment measurement, the vertical leg was clamped and the specimen was loaded in compression to a deflection of 0.5 mm at a rate of 10 mm/min. The crosshead was then returned to the initial position and the vertical leg was unclamped before taking another pair of residual moment measurements. This process was repeated at increasing 0.5 mm intervals until the measured difference in a set of P_2 measurements (no specimen and unclamped specimen) was less than 0.2 N, or the specimen collapsed. One specimen for each score group was tested for residual moment. Renman [25] used four replicates but had small variation. Our decision to use a single test was based on the nonlinearity of the *MR* data, a nonlinearity that was different for each score, and the fact that *MR* was small and that this work was exploratory. The 10 mm/min displacement rate is slightly slower than the 12.5 mm/min rate used for the BCT. **Table III** shows the crosshead travel distance and duration for each reading used for *MR* determination.

The *MR* was different for each score and changed with increased crosshead travel. A light score will have a large *MR* because the flap would like to align with the panel. A heavy score will have a small *MR* and provide little resistance to bending. Equation 5 provides the relationship between forces and *MR*. If $P_2 = 0$, then any resistance to flap closure, as determined by *MR*, gives $e < 0$, towards the outer liner. In that scenario, the panel would buckle into the box.

MR Reading	Crosshead Travel, mm	Duration, s
Start	0.0	
1st	0.5	3
2nd	1.0	6
3rd	1.5	9
4th	2.0	12
5th	2.5	15
6th	3.0	18
7th	3.5	21
8th	4.0	24
9th	4.5	27

III. Crosshead total travel and duration for MR determination.

For each eccentricity test, the vertical leg was clamped and loaded in compression at a rate of 10 mm/min. The loads P_2 and P were collected at 10 Hz and eccentricity was calculated as:

$$e = (P_2 a - MR)/(P_2 + P) \quad (6)$$

A representative eccentricity test is shown in **Fig. 6** and **Fig. 7** for the LP score on B1. Maximum P was used as the cutoff for calculation of eccentricity because P_2 would go to near 0, indicating the score line was crushed. Data was cuttoff below P = 3.5 N to ensure the horizontal leg of the specimen, the portion on the slide, was in full contact. The average of the final five values of eccentricity was recorded as e_{avg}, and the final value of eccentricity was recorded as e_{final}.

Box compression tests

The RSC boxes in each combination, with nominal dimensions 53.8-cm long, 41.6-cm wide, and 38.6-cm high, arrived knocked-down flat (KDF) on pallets and were preconditioned and conditioned following TAPPI T 402 "Standard conditioning and testing atmospheres for paper, board, pulp handsheets, and related products." Once preconditioning and conditioning were completed, boxes were assembled and sealed for testing. Flaps were bent directly to the sealing position and care was taken such that the exterior flaps were parallel and flat — an attempt to remove any "out-of-squareness." Once in position, exterior flaps were secured with shipping tape, leaving the minor flaps unrestrained. Tests were performed according to TAPPI T 804 "Compression test of fiberboard shipping containers," with ten replicates per material.

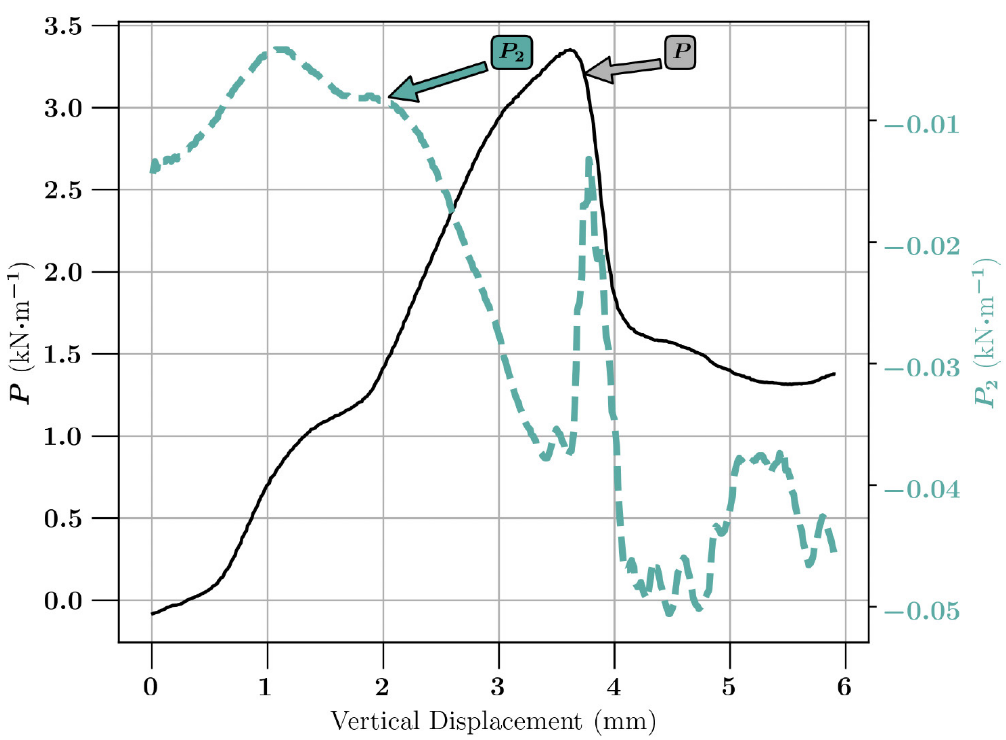

6. Example eccentricity test for a B1 LP score showing both P and P_2. Maximum P is the cutoff for calculation of eccentricity because the load is transferred from the score line to the board at that point. P_2 is in compression for the entire test. Here the maximum P is 43% of edgewise compression test (ECT).

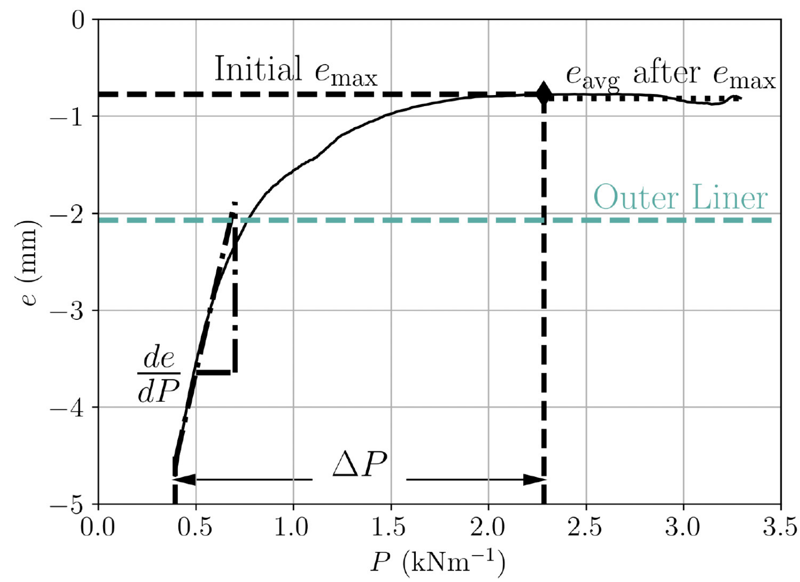

7. Example of eccentricity for a B1 LP score using the data shown in Fig. 5 and calculating e using Eq. 6 where MR was determined as described earlier. Location of outer liner is denoted.

RESULTS

This work focused on score properties for each board and its relation to BCT. **Figures 8–9** show the BCT for each board and score type. The scores in Fig. 8 are sorted in descending order by their mean BCT, and this ordering will be maintained throughout the remainder of this work, with a consistent color coding for each score. Given consistent board, differences in compression strength beyond variation in the testing can be interpreted at least in part as a function of the differences in scores. The use of two board combinations allows us to identify the consistency of any scoring impact across materials or production lots. Notched box plots provide a visual representation of the statistical analysis. On each plotted box, the middle horizontal line indicates the median, and the bottom and top edges of each box indicate the 25th and 75th percentiles, respectively. The whiskers (black lines above and below the box) extend to the most extreme data points not considered outliers. Outliers are denoted with the "○" symbol. A score with an "*" in the description indicates that the liner was cracked on the corrugator during manufacturing, prior to the test. When comparing two datasets, one can conclude with 95%

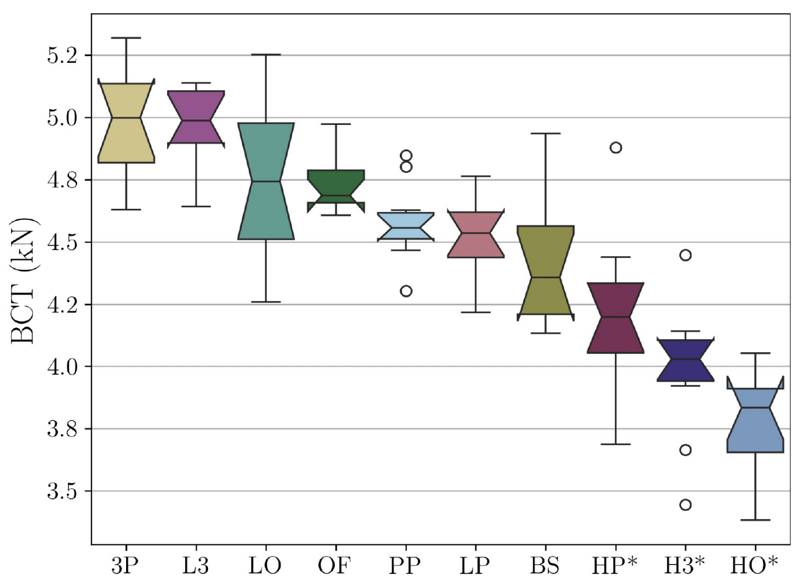

8. Box plot of box compression test strength (BCT) for B1 material. The (*) denotes liner was cracked. Materials are ordered by their BCT.

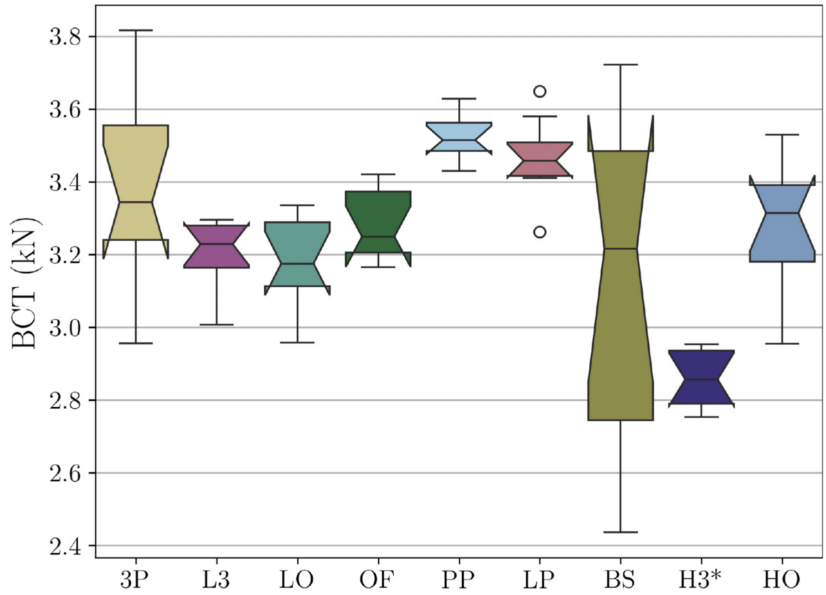

9. Box plot of BCT for B2 material. The (*) denotes liner was cracked. Materials are ordered as in Fig. 8.

confidence a true difference in median values if the notches in the box plot do not overlap. For example, the notched box plots graphically display that for B1 material, the BCT for 3P was statistically different from OF, and for B2, PP was statistically different from OF. The notched box plots also provide some indication if the values were normally distributed, as notched ends that fold back toward the median denote a skewed dataset. For example, the B1 material in Fig. 8 with score OF indicates a shortened tail on the low values of BCT.

Mean BCT and associated coefficient of variation (COV) are given in **Table IV**. Scoring appears to impact BCT, and the effect was more dramatic for B1 than for B2. As expected, score cracking significantly reduced BCT. Because they are not representative of typical production, the results for scores with cracked liners will not be included in the rest of the analysis. Cracked scoring appears to reduce the board strength by about 15% on average relative to uncracked scores, with the precise shift depending on the level of cracking and the scoring parameters.

Score	B1	B2
3P	4.98 (4.3)	3.37 (8.1)
L3	4.96 (3.3)	3.21 (2.8)
LO	4.75 (6.9)	3.18 (3.9)
OF	4.74 (2.9)	3.28 (3.0)
PP	4.56 (3.6)	3.53 (1.9)
LP	4.51 (3.7)	3.47 (3.0)
BS	4.42 (6.1)	3.13 (14.0)
HP	4.21 (7.8)	N/A
H3	3.99 (6.8)	2.86 (2.9)
HO	3.78 (5.3)	3.28 (5.1)

IV. Mean BCT (kN) and coefficient of variation, COV (%), for each board and score. Highlighted values had cracked scores.

Figures 10–11 show the moment resistance at the score as related to rotation at the score. Each curve is a single representative test chosen from all the tests of a score that had the mean K_{max} for that score. Analysis of the four-point score bending data is shown in **Table V**, with the scores ordered consistent with their BCT strengths. Variation between tests for a given score is represented by the COVs. The increased noise for rotations above 40° is caused by movement/sliding of the specimen at large rotations and because the load cell only measures force vertically while the supports are creating some horizontal forces due to friction and sliding. Most of the COVs are below 10%, which indicates small data variation. Further effort is needed to understand the effect of scoring parameters on score stiffness. This work showed that score stiffness was not consistent with BCT or across each material.

Figure 12 shows the individual eccentricity plots for material B1 for the scores 3P and PP. For most of the experiment, the eccentricity is negative, which indicates the compressive force was greater on the outer liner. For a few of the 3P scores, the load shifted to the inside liner. For the PP score, the eccentricity remained negative. Negative ec-

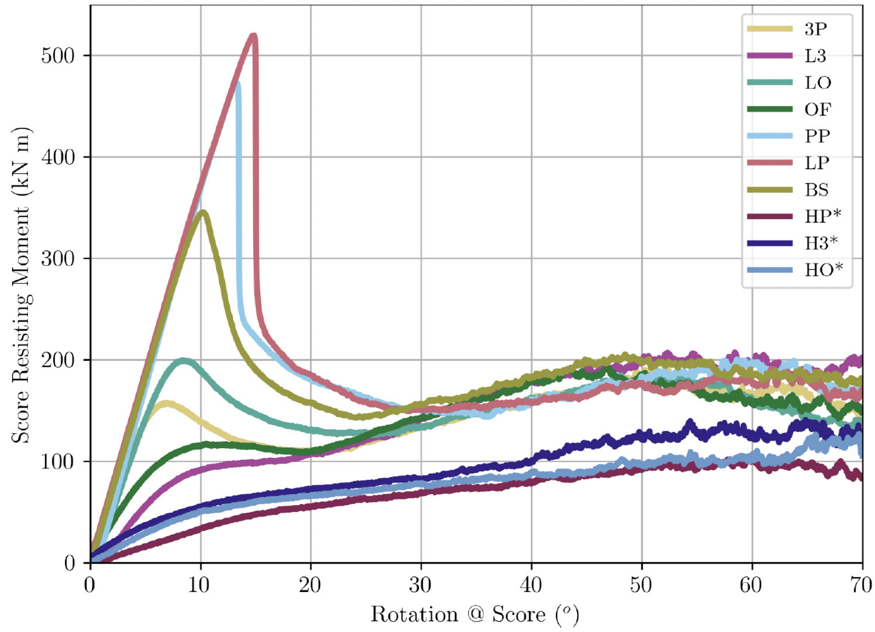

10. Example 4-point bending tests for B1 material. Selected tests were the median of the maximum moment for each score. The (*) had cracked liners at score prior to test. Parameters determined from each test are illustrated in Fig. 3.

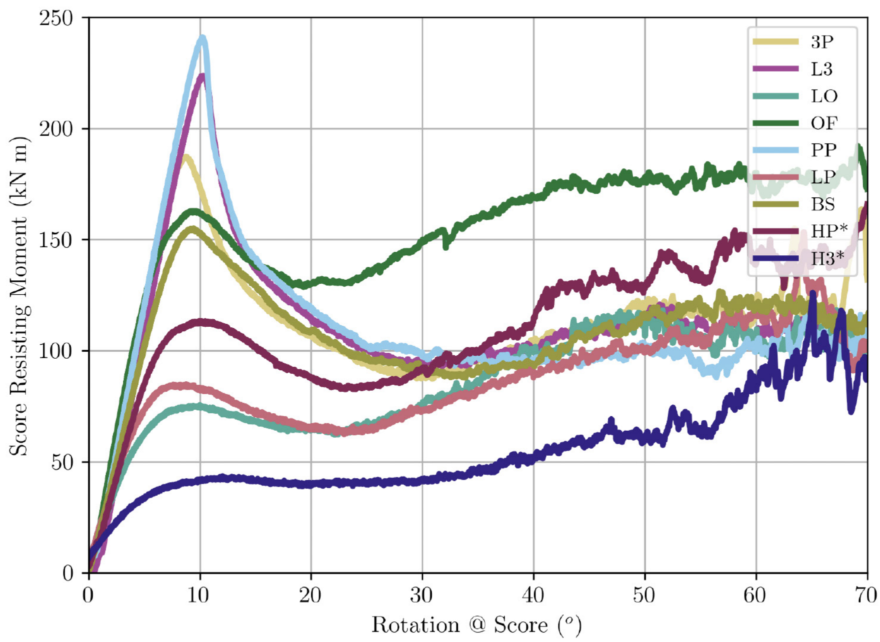

11. Example 4-point bending tests for B2 material. Selected tests were the median of the maximum moment for each score. H3* materials had cracked liners at score prior to test. Parameters determined from each test are illustrated in Fig. 3.

centricity drives the panels to buckle inward towards the box interior. For all scores of B2, the long panels buckled to the box interior and all the short panels buckled to the exterior during BCT. This buckling behavior may be related to sealing the boxes with tape, which leaves the minor flaps free to rotate and may induce different boundary conditions between the major and minor flap scores. These potential differences are part of future investigative efforts.

Table VI lists the identified parameters from the eccentricity tests on each score, which all have high COVs. Determination of *MR* was assumed to be linearly related to displacement for each board and score combination.

	Score	Stiffness, kN m/°	φK_{max}, °	K_{max}, kN m	φ @ Inflection, °	K @ Inflection, kN m	K_{45}, kN m
B1	3P	28.4 (5.5)	7.7 (9.0)	156.4 (2.9)	21.1 (4.9)	118.0 (4.3)	180.1 (4.5)
	L3	13.4 (9.5)	7.8 (18.0)	78.2 (8.4)	19.6 (2.8)	106.0 (2.7)	185.1 (3.3)
	LO	33.0 (4.0)	9.0 (5.7)	225.3 (12.4)	24.7 (4.2)	133.6 (3.1)	173.4 (2.9)
	OF	16.6 (4.5)	13.6 (9.7)	116.7 (2.4)	119.0 (3.5)	110.5 (2.3)	175.7 (5.3)
	PP	38.5 (4.8)	13.1 (4.7)	467.4 (4.2)	33.1 (5.5)	148.2 (3.9)	168.4 (3.9)
	LP	37.2 (4.3)	13.9 (10.0)	482.6 (9.9)	32.2 (7.2)	152.6 (3.2)	170.8 (4.0)
	BS	35.9 (6.3)	10.3 (4.7)	339.5 (5.1)	24.6 (4.1)	148.7 (5.3)	197.5 (6.5)
B2	3P	12.6 (8.1)	9.7 (10.1)	75.7 (4.6)	21.6 (4.0)	63.7 (4.6)	108.5 (6.4)
	L3	14.4 (10.0)	8.5 (7.3)	80.5 (6.0)	21.5 (6.4)	65.4 (4.5)	103.6 (4.0)
	LO	21.1 (3.4)	9.7 (5.5)	154.9 (4.0)	34.5 (11.5)	93.7 (4.9)	105.0 (4.1)
	OF	28.3 (4.7)	8.8 (5.4)	164.9 (5.3)	21.9 (5.0)	129.4 (4.0)	177.0 (5.6)
	PP	24.5 (3.8)	9.1 (5.1)	195.3 (9.0)	31.4 (4.1)	87.4 (3.4)	103.9 (5.1)
	LP	25.3 (2.9)	10.0 (5.2)	216.1 (7.4)	32.4 (6.2)	88.0 (4.1)	100.5 (4.0)
	BS	21.8 (6.0)	8.8 (5.6)	153.9 (9.4)	24.2 (6.0)	89.0 (3.7)	120.8 (9.1)
	HO	26.3 (2.7)	9.9 (7.7)	237.7 (7.2)	35.3 (9.9)	87.9 (7.5)	97.0 (5.0)

V. Mean score properties for each board. COV (%) is in parentheses.

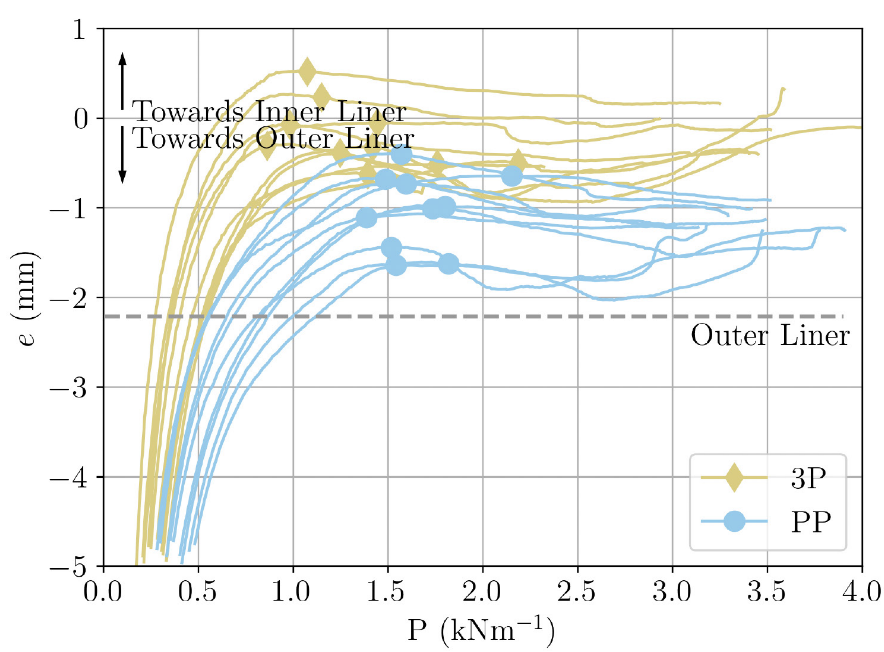

12. Eccentricity plot 3P and PP scores for B1, with e = 0 in center of the board. Markers denote initial e_{max}.

	Score	*de/dP*, mm/kNm-1	Δ*P*, kNm-1	e_{max}, mm	e_{avg}, mm	e_{final}, mm	P_{final}, kNm-1
B1	3P	20.21 (28.9)	1.09 (32.8)	-0.21 (174.6)	-0.37 (85.6)	-0.24 (136.5)	2.86 (24.1)
	L3	12.63 (27.5)	1.27 (45.2)	-1.51 (33.5)	-1.63 (26.3)	-1.64 (26.3)	2.16 (26.3)
	LO	14.27 (17.9)	1.16 (33.8)	-1.19 (19.5)	-1.22 (17.7)	-0.87 (28.6)	3.18 (8.1)
	OF	22.11 (32.0)	0.82 (27.5)	-0.97 (48.9)	-1.33 (31.9)	-1.54 (23.6)	1.73 (48.5)
	PP	8.92 (16.1)	1.29 (18.0)	-1.03 (41.8)	-1.24 (28.8)	-1.18 (12.4)	3.05 (9.6)
	LP	10.82 (32.9)	1.37 (19.9)	-0.77 (35.6)	-0.95 (26.4)	-0.77 (36.4)	2.95 (9.5)
	BS	19.93 (18.1)	1.05 (14.9)	-0.26 (163.6)	-0.42 (89.4)	-0.27 (153.3)	2.34 (19.7)
B2	B2	12.6 (8.1)	9.7 (10.1)	75.7 (4.6)	21.6 (4.0)	63.7 (4.6)	108.5 (6.4)
	3P	10.01 (15.3)	0.79 (17.7)	-1.95 (12.0)	-2.12 (9.5)	-2.12 (19.3))	1.35 (24.7)
	L3	9.98 (13.8)	0.76 (19.7)	-1.98 (16.8)	-1.99 (14.7)	-1.90 (18.2)	-1.47 (32.3)
	LO	15.17 (28.4)	0.88 (20.5)	-1.40 (15.7)	-1.58 (10.1)	-1.48 (14.5)	1.95 (15.8)
	OF	26.31 (27.7)	0.91 (31.2)	-0.16 (176.8)	0.43 (44.1)	-0.31 (115.5)	3.01 (30.3)
	PP	11.24 (23.7)	1.03 (16.4)	-1.12 (24.2)	-1.20 (16.8)	-0.99 (36.7)	2.78 (18.0)
	LP	9.59 (14.3)	0.71 (36.6)	-1.67 (26.9)	-1.68 (15.2)	-1.79 (21.7)	2.46 (12.4)
	BS	17.67 (35.0)	0.83 (28.7)	-0.96 (32.6)	-1.31 (25.6)	-1.50 (26.6)	1.48 (27.1)
	HO	15.43 (37.6)	0.95 (9.43)	-1.22 (34.3)	-1.25 (25.5)	-1.05 (38.5)	2.44 (23.9)

VI. Eccentricity analysis showing mean values. COV (%) is in parentheses.

Equation 6 demonstrates that *MR* is the sole contributor to *e* during initial compression ($P_2 = 0$). As such, initially $e < 0$ and buckling is toward the box interior. As the compression increases, *e* approaches zero or, possibly, becomes positive. This change of *e* indicates the boundary condition is changing, but it is unclear whether the inward panel deflections caused by *MR* were ever overcome. In the BCT performed in this work, all long-side panels failed toward the interior and most short-side panels failed to the exterior (all except four boxes with different scoring). For the long-side panels, the concave failure produced a “smile crease” on the outside, which is not a common failure observed in practice. We were unable to determine whether this type of failure was created by our box closure method (taping) or the result of testing an empty box that allowed the initial eccentricity to instigate a buckling mode. Our observation during testing was that long-panel buckling towards the interior was dominant and caused exterior buckling in the short panels. Future work is planned to improve the measurement of MR_0 and better assess the evaluation approach. Interestingly, in this experiment, eccentricities for all scores were negative.

Figure 13 shows mean DST for each score type and for each board. The “NS” refers to unscored specimen. Scoring reduced DST for all profiles and indicated a damage metric for each score that showed similar trends for each board. Data variation was small enough to indicate real differences between score profiles, but no consistent correlation with BCT. Figure 4, the schematic of the DST specimen, shows the score line centered vertically within the specimen. Accurate centering of the score line on the neutral axis of the specimen is important because the measurement requires a symmetric specimen; however, offset scores, like LO and OF, are not symmetric through the thickness, and their response is subject to asymmetry. Also, due to the complexity of accurately determining *I* for scored specimens (Eq. 3), we chose to assume, albeit incorrectly, that *I* was constant both across different scoring profiles and within a particular scoring profile. The DST measurements are minimally affected by small *I* differences, which indicates that the differences in loss of torsional stiffness are caused by differences in score mechanical behavior. The damage intentionally created by the score is symmetric across the width of the specimen for some scores, for ex-

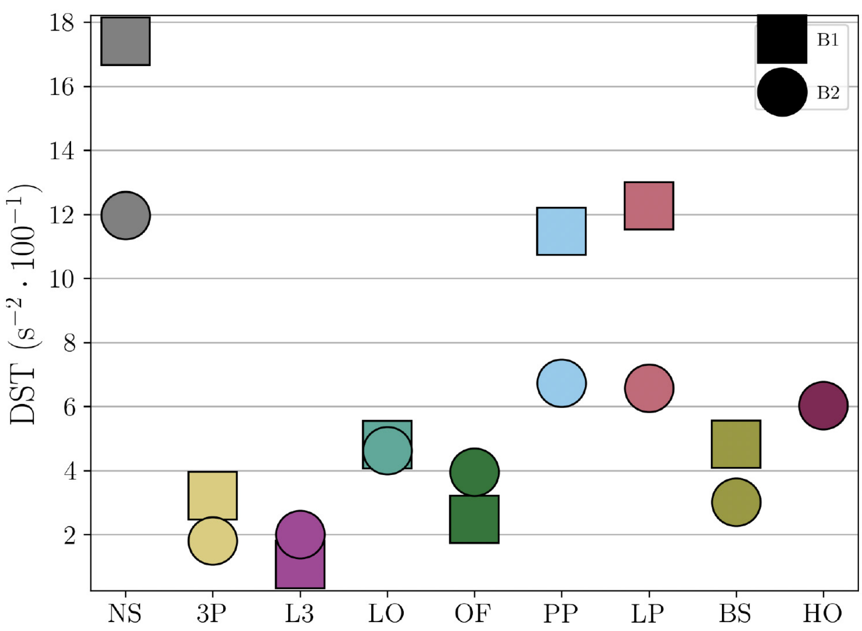

13. Mean DST for each board and score. The "NS" refers to unscored specimens. The B1 scores had higher DST than B2, except for score OF. Only B2 HO is shown, because that score was cracked for B1. Typical data range was on the order of marker size.

ample 3P and PP, but not for other scores, for example OF and LO. Effect of non-symmetry of the score on DST is outside the scope of this exploratory effort. Finally, damage caused by the score had different widths, depending on score geometry, and score depths were varied. Each of these contribute to reduction of DST. These concerns further limit any meaningful correlation between DST of the score and BCT values.

Since the testing procedures described in this work are destructive, it is not possible to obtain paired data. That is, it is not possible to obtain both BCT values and eccentricity or bending or torsion results for the same specimen. For this reason, traditional regression, or other direct correlation-detecting methods, cannot be applied. Therefore, we have applied a method to obtain simulated paired data. This was achieved in the following way: For any given predictor variable, say K_{max}, we randomly selected a single observation of K_{max} and one BCT observation from each applicable score type to obtain a collection of points, or paired observations. We then were able to apply simple linear regression to these data, resulting in an R value representative of correlation between data. Repeating this process 1000×, we obtained a sample of R values, from which we were able to obtain an estimate of the R value (correlation coefficient) by taking the sample mean. A sample size of 1000 sufficiently captures a reasonable estimate of the actual R. Here we use R, instead of R_2, to illustrate the negative correlation for an inverse relationship between parameters. **Table VII** depicts the results for a selection of predictor variables. While K_{max} did have the largest R value, that value is still small. The K_{max} was a better predictor of B1, because B2 did not have significant differences in BCT.

Test	Predictor Variable	Mean R
4-Point bending	K_{max}	-0.596
	φK_{max}	-0.461
DST	TQ	-0.492

VII. Three highest absolute R values for the predictor variables of BCT.

The predictive capacity of ΔP, e_{max}, and K_{45} on BCT were negligible, but φK_{max} and K_{max} do suggest further study and investigation may be warranted. While the determination of eccentricity variables were not good predictors in this exploratory effort, we plan to continue to gather eccentricity data on a larger variety of board constructions. The presence of interactions across the explanatory variables was not assessed but should be considered in a more comprehensive study.

CONCLUSIONS

In this exploratory effort, two board constructions were used to examine the effect of score parameters on BCT. One of the two constructions had BCT differences of 10% across the range of scores studied. The score evaluation tests, four-point bending, eccentricity, and DST had minimal predictive ability for the impact of the score profile on box strength. However, this was not unexpected, as small differences in BCT should correspond to small differences in predictive tests. Comparing score bending test results across multiple corrugated boards is needed to more completely appraise its predictive value. The presence of interactions across the explanatory variables was not assessed but should be considered in a more comprehensive study.

That scoring parameters created BCT differences that were not strongly predicted by standard tests in the current study suggests other tests may be needed to examine the actual boundary conditions at the top and bottom platens during BCT. Boundary conditions may evolve and change during the test as incremental failures occur in the score line, which likely led to the limited effectiveness of eccentricity data in the statistical BCT model. Also, other constructions may have larger BCT differences due to scoring, and these predictive tests may be more useful. Direct examination of the boundary conditions incorporating other constructions will be the focus of future work.

FINANCIAL DISCLOSURE

This work was funded by the Fibre Box Association through a Cooperative Research and Development Agreement #22-RD-11111122-004 with USDA, Forest Service, Forest Products Laboratory.

LITERATURE CITED

1. Global Market Insights, “Corrugated packaging market size," Technical Report, Global Market Insights, Selbyville, DE, USA, 2024.
2. McKee, R.C., Gander, J.W., and Wachuta, J.R., *Paperboard Packag.* 48(8): 149(1963).
3. “A comparison of box and tube top-load compressive strength,” Testing Compression Report 1, Institute of Paper Chemistry, Appleton, WI, USA, 1946.
4. Kloth, G.R. and Fox, T.S., “Study of the effect of different scoring techniques and scoring profiles on box compression performance,” Project 2695-19, Technical Report, Institute of Paper Chemistry, Appleton, WI, USA, 1977.
5. McKee, R.C. and Gander J.W., *Tappi* 40(1): 57(1957).
6. Angell, B.S. and Paslay, P.R., *Tappi* 42(6): 194A(1959).

ABOUT THE AUTHORS

This topic has been mentioned many times in the past by packaging scientists as an important area of research. Recent equipment development made this study possible, a development allowing online scoring changes on the corrugator. Most of our work involves the physics of packaging papers and structures made from them. This investigation was waiting for equipment improvements so that the scoring would not be done in the laboratory, often called cold scoring, but on the corrugator instead.

The parameter space describing scoring variables is immense, so the most difficult aspect of this study involved choosing how to limit that space. We received excellent guidance from the Fibre Box Association Technical Committee.

In this exploratory work, we examined the effect of scoring parameters on box compression strength of two balanced boards. We found that the scoring effect was not the same across the boards. We also found that scoring does affect box compression strength, so much work is needed.

This work will be helpful to those operating corrugating plants. Besides employing particular scoring parameters for flap opening and closing operations, parameters may be optimized to improve box compression strength.

Current work suggests that some score tests are predictive for box compression tests. As a next step, those tests need to be investigated by examining additional board geometry and scoring parameters.

Considine is Materials Research engineer; Bechle is Materials Research engineer; Bridwell is general engineer; Arvantis is Mathematical statistician; and Tang is Materials Research technician at the USDA Forest Service Forest Products Laboratory in Madison, WI, USA. Frank is director, Materials Research and Innovation, at the PCA Research and Innovation Center in Vernon Hills, IL, USA. Email Considine at john.m.considine@usda.gov.

Considine

Bechle

Bridwell

Arvantis

Frank

Tang

7. Kutt, H. and Mithel, B.B., *Tappi* 51(4): A79(1968).
8. Garbowski, T., Gajewski, T., and Knitter-Piątkowska, A., *Sensors* 22(13): 4800(2022). https://doi.org/10.3390/s22134800.
9. Urbanik, T.J. and Frank, B., *Wood Fiber Sci.* 38(3): 399(2006).
10. Koning, J.W. and Laundrie, J.F., "Packaging perspective, 1910-1985," General Technical Report, USDA Forest Products Laboratory, Madison, WI, USA, 1985. https://doi.org/10.2737/FPL-GTR-51.
11. Frank, B., *Packag. Technol. Sci.* 27(2): 105(2014). https://doi.org/10.1002/pts.2019.
12. Maltenfort, G.G., *Paperboard Packag.* 65(9): 71(1980).
13. Peterson, W.S. and Schimmelpfenning, W.J., *Tappi* 65(8): 108(1982).
14. Bijlaard, P.P., *J. Aeronaut. Sci.* 17(11): 742(1950). https://doi.org/10.2514/8.1788.
15. Nordstrand, T.M., *Compos. Struct.* 30(4): 441(1995). https://doi.org/10.1016/0263-8223(94)00066-2.
16. Cillie, J. and Coetzee, C., *Math. Comput. Appl.* 27(6): 108(2022). https://doi.org/10.3390/mca27060108.
17. FBA & PMMI, "Tolerances for regular slotted containers (RSCs)," PMMI B155-TR2.1-2018, Technical Report, Packaging Machinery Manufacturers Institute/Fibre Box Association, Herndon, VA, USA/ Itasca, IL, USA, 2018.
18. Nagasawa, S., Fukuzawa, Y., Yamaguchi, T., et al., *J. Mater. Process. Technol.* 140(1-3): 157(2003). https://doi.org/10.1016/S0924-0136(03)00825-2.
19. Chin, S.M., Youn, H.J., and Lee, H.L., *J. Korea TAPPI* 41(1): 44(2009).

ABOUT THIS PAPER

Cite this article as:
Considine, J.G., Bechle, N.J., Bridwell, J.J., et al., *TAPPI J.* 25(8): 493(2026). https://doi.org/10.32964/TJ25.8.493

DOI: https://doi.org/10.32964/TJ25.8.493

ISSN: 0734-1415

Publisher: TAPPI Press

About this journal

20. Nagasawa, S., Bin, M.N., and Shiga, Y., *J. Adv. Mech. Des. Syst. Manuf.* 5(4): 385(2011). https://doi.org/10.1299/jamdsm.5.385.
21. Huang, H. and Nygårds, M., *Nord. Pulp Pap. Res. J.* 26(4): 452(2011). https://doi.org/10.3183/npprj-2011-26-04-p452-467.
22. Nagaswa, S., Takamatsu, T., Fukuzawa, Y., et al., *AIP Conf. Proc.* 1315: 1017(2011). https://doi.org/10.1063/1.3552312.
23. Lindbladh, J., "Development of a 4-point bending test to characterize creases on paperboard and packaging material," Master's thesis, Lund University, Lund, Sweden, 2018.
24. Chalmers, I.R., *Appita* 59(5): 357(2006).
25. Renman, M., *Exp. Mech.* 36(3): 262(1996). https://doi.org/10.1007/BF02318017.